

# Nanoelectromechanics of Inorganic and Biological Systems: From Structural Imaging to Local Functionalities

Brian J. Rodriguez,<sup>1,2</sup> Sergei V. Kalinin,<sup>1,2</sup> Stephen Jesse,<sup>1</sup> G. Thompson,<sup>3</sup> A. Vertegel,<sup>3</sup> Sophia Hohlbauch,<sup>4</sup> Roger Proksch<sup>4</sup>

<sup>1</sup>Materials Science and Technology Division and <sup>2</sup>The Center for Nanophase Materials Sciences, Oak Ridge National Laboratory, Oak Ridge, TN

<sup>3</sup>Clemson University, Department of Bioengineering, Clemson, SC

<sup>4</sup>Asylum Research, Santa Barbara, CA  
sergei2@ornl.gov

Coupling between electrical and mechanical phenomena is extremely common in inorganic materials, and nearly ubiquitous in biological systems, underpinning phenomena and devices ranging from SONAR to cardiac activity and hearing. This paper briefly summarizes the Scanning Probe Microscopy (SPM) approach, referred to as Piezoresponse Force Microscopy (PFM), for probing electromechanical coupling on the nanometer scales, and delineates some existing and emerging applications to probe local structure and functionality in inorganic ferroelectrics, calcified and connective tissues, and complex biosystems based on electromechanical detection.

Electromechanical coupling includes a broad class of phenomena in which an electrical stimulus elicits a mechanical response (e.g., deformation), or a mechanical stimulus elicits an electrical response. The simplest example of electromechanical coupling is piezoelectricity, or a linear relationship between the applied force and the induced charge (in the case of the direct piezoelectric effect), or the applied bias and resultant strain (converse piezoelectric effect). Considering that 20 out of 32 crystallographic point groups and virtually all optically-active biopolymers containing polar functional groups are piezoelectric, it is no wonder that electromechanics is all around us. Another, more complex example of electromechanical coupling is flexoelectricity (coupling between the electric field and the strain gradient), which is ubiquitous in liquid crystals and cellular membranes and plays a key role in function of hearing cells (conversion of acoustic waves of audible sound into neural electrical signals), and energy storage in mitochondria. Finally, biological systems offer an endless variety of even more complex electromechanical behaviors.

For more than 60 years, electromechanical coupling in piezoelectric crystals such as quartz and ferroelectric perovskites was utilized in devices and applications such as SONAR and ultrasound imaging.<sup>1</sup> The progress in materials and device fabrication in the last several decades has brought about a gamut of novel applications, including sensors, actuators, microelectromechanical systems (MEMS) and surface acoustic wave devices (SAW).<sup>2</sup> Ferroelectric materials, a subclass of piezoelectrics

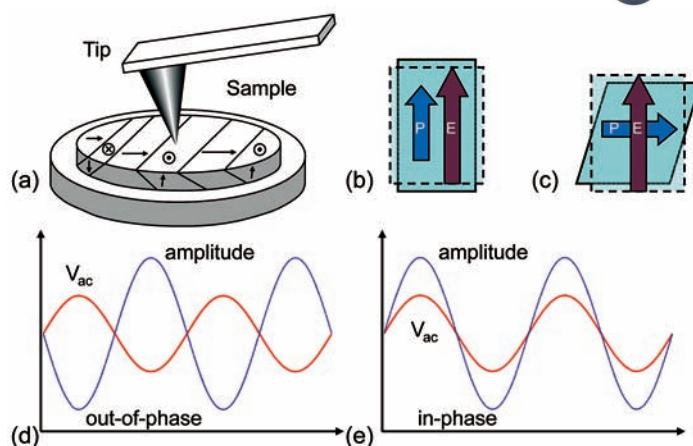


**Fig. 1.** (a) Schematic of the PFM experimental setup. (b) Ferroelectric domains with polarization oriented perpendicular to the sample surface will expand and contract with applied bias, leading to a sample deformation that can be measured as a tip-deflection (VPFM). (c) Ferroelectric domains with polarization oriented parallel to the sample surface will shear, and can be detected via the torsion of the cantilever (LPFM). The amplitude of the deflection and the torsion is related to the magnitude of the piezoelectric coupling coefficients, while the phase response provides information about the polarization orientation. In VPFM, the phase signal is (d) out-of-phase with the driving signal when the applied field is anti-parallel to the polarization direction, and (e) in-phase when they are parallel [as shown in (b)].

with switchable polarization, are rapidly emerging as materials for non-volatile ferroelectric memories (e.g. in smart cards and Sony Playstations),<sup>3</sup> ferroelectric data storage, non-volatile gates for field-effect transistors, and tunneling barriers. In biological systems, electromechanical coupling manifests itself in virtually all aspects of biological activity – from neural control of muscular activity known since the time of Luigi Galvani to the function of electromotor proteins and voltage-gated ion channels, which

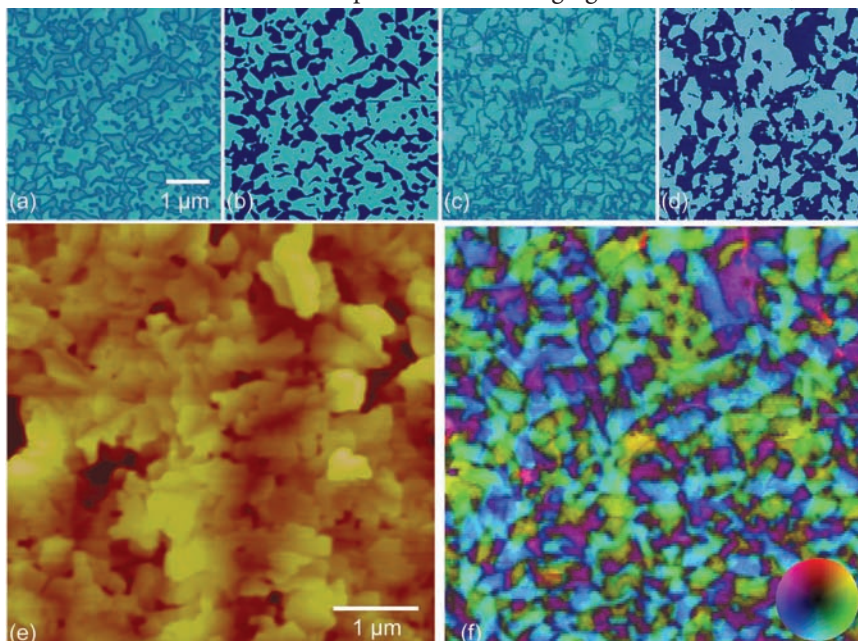


**Fig. 2.** (a,b) Vertical and (c,d) lateral PFM (a,c) amplitude and (b,d) phase images, respectively, of a BFO film. (e) Topography of the same region. (f) Vector PFM image of the combined vertical and lateral images. The orientation angle is coded by the color as reflected in the “color wheel” legend, while the intensity provides the magnitude of the response (dark for zero response, bright for strong response). The vertical range is 20 V for (1-d) and 20 nm for (e). (a,b) were measured using a bias of 1 V at 1.3 MHz, while (c,d) were recorded using a bias of 5V and a frequency of 12 kHz. Sample courtesy of Y.H. Chu and R. Ramesh (UC Berkeley).

# Side-By-Side Comparison? Difficult When Our Coaters Stand Alone.



## High Resolution Sputter Coater 208HR for FE-SEM

### Superior Features:

- High Resolution Fine Coating
- Wide Choice of Coating Materials
- High Resolution Thickness Control
- Multiple Sample Stage Movements
- Wide Range of Operating Pressures
- Compact, Modern, Benchtop Design



Find out about our complete line of sample coaters.

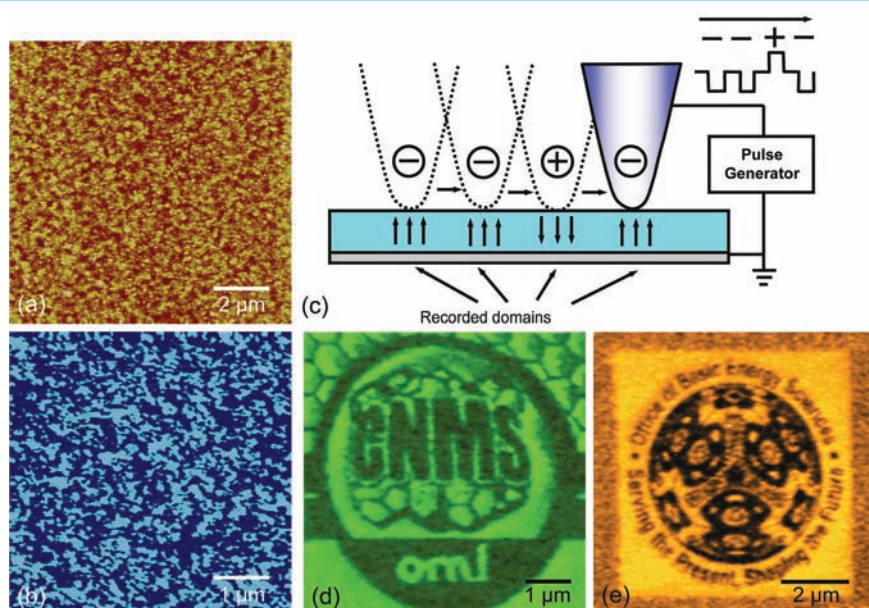


**Fig. 3.** (a) Topography image of a PZT film, and (b) representative PFM phase image of a smaller area showing the as-grown domain structure. (c) Schematic demonstrating the principle of ferroelectric lithography. (d,e) Two examples of ferroelectric domain writing. The recorder pattern represents polarization in the sample visualized by PFM, and does not affect surface topography in contact mode AFM. The vertical scales for (a) and (d) are 10 nm and 20 V, respectively. For (d,e) a mixed piezoresponse (PR) signal representation,  $R = A \cos \phi$ , is used, where  $A$  is the PFM amplitude and  $\phi$  is the PFM phase. Sample courtesy of S.-H. Kim (Inostek).

are being studied only now. To drive electromechanical and ferroelectric device development and to understand the biological significance of electromechanical coupling in biosystems (e.g. to improve the functionality of artificial biomaterials), it is necessary to probe electromechanics on the length scales from microns to nanometers, and ultimately down to the level of a single unit-cell or protein molecule.

Scanning probe microscopy provides an ideal platform for such measurements, as it combines nanoscale resolution with the capability to perform both electrical and mechanical stimulations and measurements. In particular, PFM allows electromechanical activity to be probed directly on the nanoscale by measuring the mechanical response to an electrical field applied via a conducting tip with a sensitivity of  $\sim 1 \text{ pm/V}$ .<sup>4</sup> Here, we describe the implementation of PFM to probe electromechanical coupling in inorganic and biological systems on the nanoscale, and delineate its applications for structural and functional imaging.

The central paradigm of PFM is similar to conventional atomic force microscopy (AFM) in that it involves a sharp conductive tip mounted on a cantilever. The tip acts as a local probe interacting with the surface, while the cantilever acts as a force sensor detecting forces exerted on the tip. An illustration of the PFM experimental setup is shown in Fig. 1 (a). A bias,  $V_{tip} = V_d + V_a \cos(\omega t)$ , is applied to a conductive AFM tip in contact with a sample. The applied ac bias will cause a piezoelectric material under the tip to expand and contract in the vertical direction [Fig. 1(b)], or shear, resulting in lateral surface displacement [Fig. 1(c)]. This deformation is detected via the AFM cantilever as the first harmonic component of the bias-induced tip deflection,  $d_{10} \cos(\omega t + \phi)$ , as shown in Fig. 1(d,e). The response amplitude,  $d_{10}$ , provides a measure of the local electromechanical activity of the surface.

For the past decade, PFM has emerged as a tool for nanoscale characterization of ferroelectric materials.<sup>5</sup> In ferroelectrics, PFM can be used to visualize ferroelectric domains, since the piezoelectric response depends on the polarization magnitude and direction. The phase of the piezoresponse,  $\phi$ , yields information on the polarization direction below the tip. For example, when the applied field is parallel to the polarization direction [Fig. 1(b)], the phase of the piezoresponse is in-phase with the driving signal [Fig. 1(e)]. The signal will be out-of-phase when they are anti-parallel [Fig. 1(d)]. The out-of-plane polarization is measured by recording the tip-deflection signal at the frequency of modulation, and is generally called vertical PFM (VPFM). PFM is also sensitive to in-plane polarization. The in-plane component of polarization can be detected as the torsion of the cantilever due to the bias-induced surface shearing [Fig. 1(c)], and is typically called lateral PFM (LPFM).

The VPFM and LPFM data can be combined to reconstruct the real-space polarization orientation.<sup>6</sup> VPFM and LPFM amplitude and phase images of a bismuth ferrite (BFO) surface are shown in Fig. 2. When the amplitude response is strong, it corresponds with a region of strong electromechanical activity. The vertical response for a domain oriented completely out-of-plane will be larger than that for a domain with some lateral component of polarization. Similarly, the lateral response will be larger for a domain with polarization oriented completely in-plane, and zero for a domain oriented completely out-of-plane. Domains with different out-of-plane (or in-plane) polarizations will be separated by a region of null response, corresponding to a

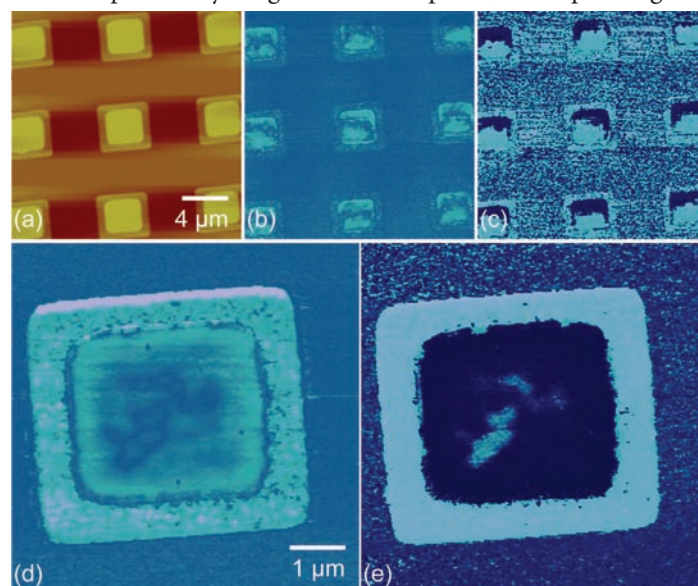


**Fig. 4.** (a) Topography, (b) PFM amplitude, and (c) PFM phase images of an array of ferroelectric capacitors. (d,e) PFM amplitude and phase images of one of the capacitors after the application of a switching bias. The domain structure of exposed film (ridge) and material below the electrodes (central area) are clearly seen. The vertical data scales are 1  $\mu\text{m}$ , 10 V, and 20 V for (a-c), respectively. Sample courtesy of S.-H. Kim (Inostek) and S.-K. Hong (Hynix Semiconductor).

MBL

Biological Discovery in Woods Hole

Founded in 1888 as the Marine Biological Laboratory

## 2008 Microscopy Courses

### ANALYTICAL & QUANTITATIVE LIGHT MICROSCOPY

May 7 - May 16, 2008      Application Deadline: January 23, 2008

This comprehensive course provides an in-depth examination of the theory of image formation and the application of video methods for exploring subtle interactions between light and the specimen.

### OPTICAL MICROSCOPY & IMAGING IN THE BIOMEDICAL SCIENCES

October 7 - October 16, 2008      Application Deadline: June 27, 2008

This course will enable the participant to obtain and interpret microscope images of high quality to perform quantitative optical measurements and to produce video and digital records for documentation and analysis.

For further information & applications, visit:  
[www.MBL.edu/education](http://www.MBL.edu/education)

or contact: Admissions Coordinator  
[admissions@mbi.edu](mailto:admissions@mbi.edu), (508)289-7401

The MBL is an EEO/Affirmative Action Institution.

## The New Dual Standard.

Our 3Max™ Dual SEM ETD simultaneously detects both SE and BSE using SE3 collection.

Even at 250 eV.



### It's an EI-Mul.



### EI-Mul

<http://www.el-mul.com>

Electron & Ion  
Detection Solutions

### You can detect *the difference.*

Custom Microscopy Supplies  
From  
M. E. Taylor Engineering, Inc.

## New SEM Scintillator LuminiX ScintillatoR (LXSR)

- Single crystal = long life
- Brighter than YAP or YAG
- Peak emission 420nm
- Decay constant 35ns
- Any diameter or thickness
- Made in the USA
- Fast delivery

Phone (301) 774-6246

See our products on the Web @  
[www.semsupplies.com](http://www.semsupplies.com)

INDUSTRY ■ RESEARCH ■ MEDICINE

## WETSEM<sup>®</sup>

BREAKTHROUGH TECHNOLOGY

- High Resolution Imaging of Fully Hydrated Samples
- Greatly Reduces Prep Time
- Capsule Fits Standard SEMs
- Safe and Simple to Use



QX-102



QX-202



QX-302

<http://www.quantomix.com>

# QUANTOMIX<sup>®</sup>

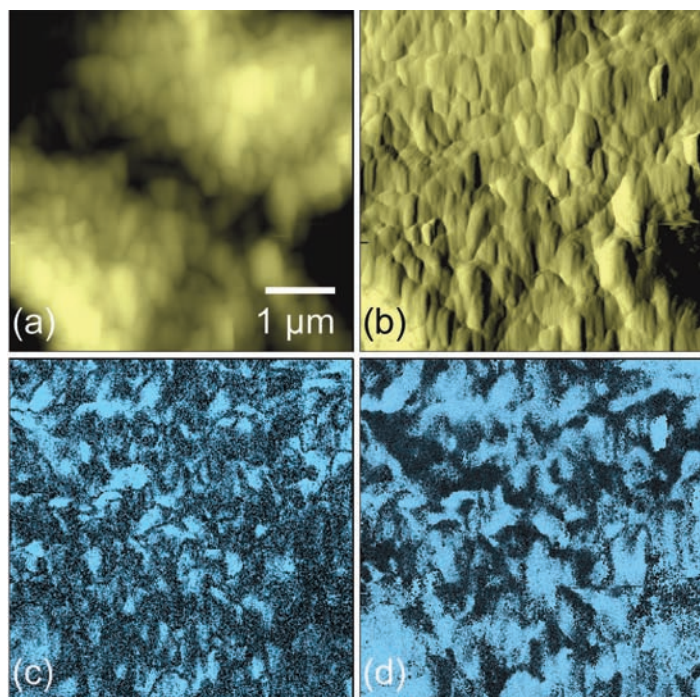


**Fig. 5.** (a) Topography, (b) deflection, (c) PFM amplitude, and (d) phase images of human tooth dentin. The vertical data scales are 350 nm, 10 nm, 50 pm, and 180° for (a-d), respectively. Sample courtesy of S. Habelitz (UC San Francisco).

domain wall. The width of the domain wall is typically related to the geometric size of a tip, since for most materials ferroelectric domain walls are atomically sharp (below 1 nm width). In order to visualize the differences between in- and out-of-plane polarizations, the 3D orientation of the polarization can be reconstructed from the vertical and lateral images. The combined vector PFM image is shown in Fig. 2(f). The orientation angle is coded by the color as reflected in the “color wheel” legend [Fig 2(f)], while the intensity provides the magnitude of the response (dark for zero response, bright for strong response).

So far, we have considered PFM as a tool for measuring the existing polarization state and mapping the electromechanical activity. PFM can also be used to modify the ferroelectric polarization through the application of a bias, as illustrated in Fig. 3.

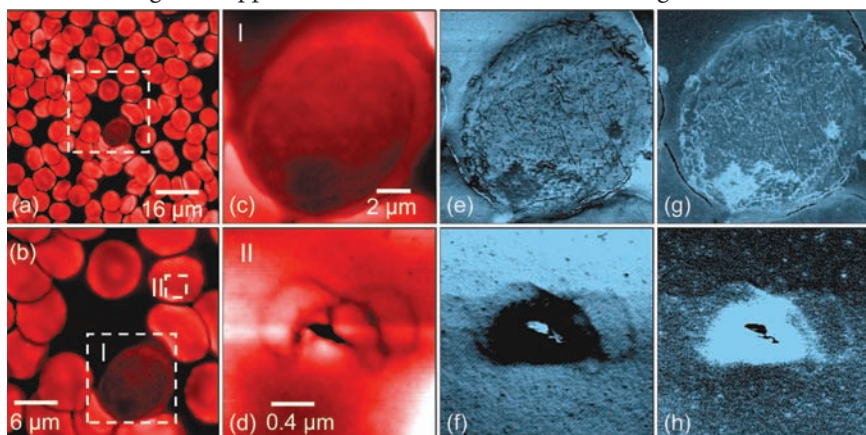


**Fig. 6.** (a,b,c,d) Topography images of blood cells with decreasing scan size. A white blood cell in the center of Fig. 6a appears darker than the surrounding numerous red blood cells. Electromechanical (e) amplitude and (g) phase images of the white blood cell in (c) [Region I in (b)]. Electromechanical (f) amplitude and (h) phase images of a structural feature (d) on a red blood cell [Region II in (b)]. The vertical data scales are 1 μm for (a,b,c), 50 nm for (f), 800 pm for (d), 5° for (e), 400 pm for (g) and 1° for (h).

When the applied field is large enough (e.g. greater than the local coercive field) it can induce ferroelectric polarization reversal. This technique can be used to ‘write’ single domains, domain arrays, and complex patterns. Consider the topography image shown in Fig. 3(a). The as-grown domain structure is shown in Fig. 3(b), a PFM phase image of a region half the area of Fig. 3(a), which reveals an initial random domain orientation. By applying a bias to certain regions as shown in Fig. 3(c), it is possible to switch the polarization in some places so that certain regions are oriented ‘up’ while others are oriented ‘down.’ By controlling the bias carefully, it is possible to ‘write’ patterns. In Fig. 3(d,e) the logos for the Center for Nanophase Materials Sciences (CNMS) at ORNL and the Department of Energy Office of Basic Energy Sciences have been patterned into a ferroelectric film via ferroelectric lithography. The patterns are written without changing the surface topography [Fig. 3(a)]. The ultimate limit for this writing process is determined by the material properties and the sharpness of the tip, and under optimal conditions reliable fabrication of 5–8 nm features (bit size for information storage) has been demonstrated.<sup>7</sup> Notably, surface polarization controls chemical reactivity of the surface in the acid dissolution and metal photodeposition processes, providing a pathway to transform the polarization pattern into topographic or deposited metal pattern.<sup>8</sup>

PFM can also be implemented through a thin conducting layer. This allows for nanoscale characterization of FeRAM and other ferroelectric devices. In this case, the applied field is uniform beneath the top electrode, and local switching properties can be investigated independently from changes in the tip-sample electrical contact. Examples of electromechanical imaging of ferroelectric capacitors are shown in Fig. 4. In this case, the film in-between the capacitors has been etched away, so that only the capacitors themselves reveal the domain structure.

Recently the reach of PFM has been extended beyond ferroelectrics to piezoelectric semiconductors, polymers, and biopolymers.<sup>9,10,11</sup> PFM images of human tooth dentin are shown in Fig. 5. The regions with different response can be clearly seen on the PFM amplitude and phase images [Fig. 5(c,d)], providing insight into internal structure of this tissue on the sub-10 nanometer level beyond the resolution of surface topographic image.

While the functional origin of observed contrast is still under investigation (e.g. direction of electromechanical response is tied with local molecular orientation), this method allows high resolution structural imaging of the tissue by distinguishing piezoelectric proteins from the non-piezoelectric hydroxyapatite matrix.

One might expect that virtually all biosystems manifest a mechanical response to an applied bias. Other phenomena may contribute to the observed signal (e.g. flexoelectricity) and may provide some structural and functional insight into the material being studied. Recently, we have attempted PFM on biological systems such as cells. A panel of topography and electromechanical images of blood cells are shown in Fig. 6. There is a remarkable contrast in the electromechanical images of the white blood cell in Fig 6 (e-h). While the origin of this contrast

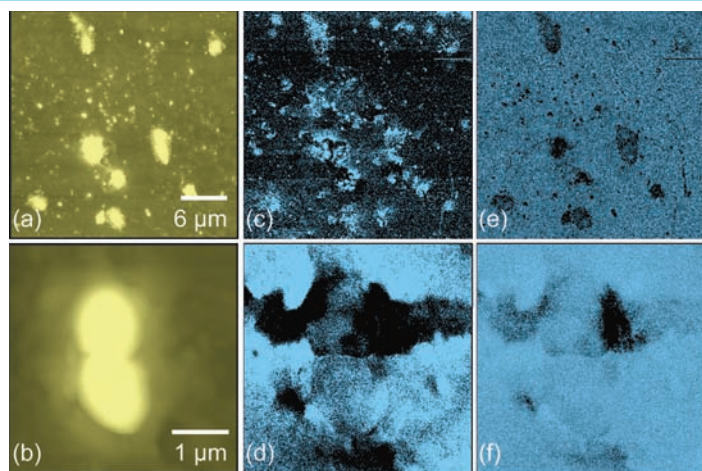


**Fig. 7.** (a,b) Topography and (c,d) PFM amplitude and (e,f) phase images of yeast cells in ambient. The vertical data scales are 115 nm for (a), 437 nm for (d), 1 V for (b,e), and 5V for (c,f).

is open to interpretation, it does reveal some information about the cell that is not visible in topography or deflection (not shown) images. Interestingly, features are visible on red blood cells as well, which generally coincide with topographic features on the cell. Further studies are needed to understand the exact signal formation mechanism, and hence the origins of observed contrast in terms of cell structure and functionality.

Another example are yeast cells imaged in air. Topographic and electromechanical images of yeast cells are in Figure 7. There is a significant increase in piezoelectric activity in the vicinity of the yeast cells (regions that are anticipated to be the last to dry). This contrast can be attributed both due to residual sugars from growth media and to the polysaccharides and glycoproteins that make up the yeast cell wall. Ideally, the observation of changes in

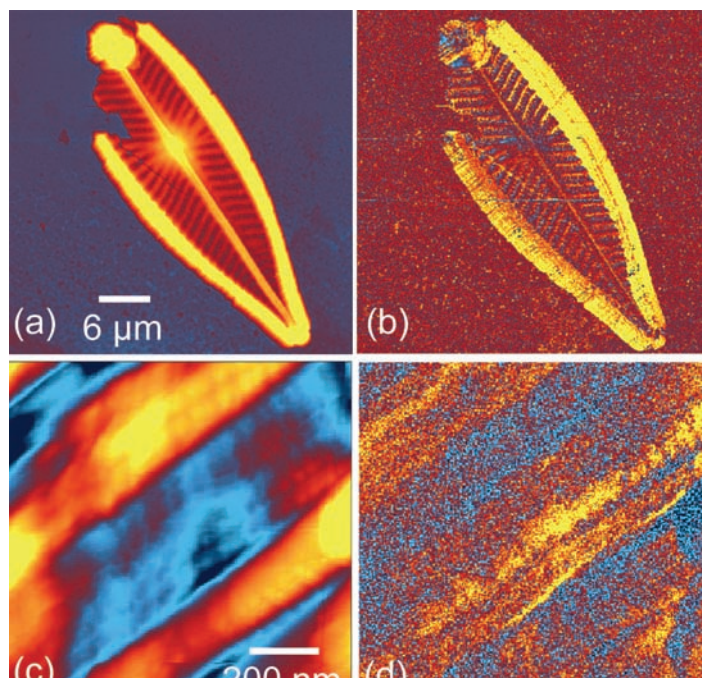


**Fig. 8.** Topographic and PFM imaging of a diatom skeleton, *Navicula radiosa*. (a,b) Topography and PFM amplitude of the entire skeleton; (c,d) topography and PFM amplitude of a zoomed-in section of a frustule ridge. The vertical data scales are 1.02 μm for (a), 600 pm for (b), 85 nm for (c) and 200 pm for (d). Diatom (*Navicula radiosa*) sample provided by Bob Janisch and Matt Julius, St. Cloud State University.

electromechanical activity in a viable cell may provide insight into biological processes at the nanoscale.

Finally, as with many other microscopic techniques, PFM at times provides truly spectacular images of the nanoworld. Shown in Fig. 8 are PFM images of the skeleton of a *Navicula radiosa*, a common benthic pennate diatom, which is a single-celled organism with a silica shell (frustule). PFM of entire frustules appeared to exhibit only topographical crosstalk from the high aspect ratio features [Fig. 8 (a,b)], but upon zooming in on the ridge of the frustule, additional features can be seen in the PFM amplitude image [Fig. 8 (d)] that are not present in the topography image [Fig. 8 (c)].

To summarize, PFM is well-established as a powerful tool to explore polarization-related phenomena in ferroelectric materials, and is quickly emerging as a powerful tool for exploring local electromechanical phenomena in biological systems. The smallness of electromechanical coupling in biopolymers (10-100 times smaller than ferroelectrics) and stringent requirements of PFM spectroscopy has necessitated the development of several schemes to improve the signal-to-noise ratio, including resonance-enhancement, dual-excitation, and high-voltage PFM. Future work in this area will require careful studies in controlled physiological environments and the development of novel modulation schemes and probe designs in order to elucidate the mechanisms of the electromechanical coupling on the nanoscale and tie it in with biological functionalities. ■

Research sponsored in part by the Division of Materials Sciences and Engineering (SVK, BJR, and SJ), Oak Ridge National Laboratory, managed and operated by UT-Battelle, LLC for the Office of Basic Energy Sciences, U.S. Department of Energy. The authors (BJR, SVK) are also grateful for financial support from Asylum Research and for the use of their imaging facilities. Samples from R. Ramesh were provided through the support of an LBL LDRD. GT and AV are also thankful to CNMS user program (projects CNMS-2005-075 and CNMS-2006-049) and NSF (CMS-0619739).

PFM and other SPM modes are available as a part of the user program at the Center for Nanophase Materials Sciences (CNMS), [www.cnms.ornl.gov](http://www.cnms.ornl.gov).

## References

- 1 Lines ME, Glass AM. 1977. *Principles and Applications of Ferroelectric and Related Materials*. Oxford: Clarendon Press
- 2 K. Uchino, *Ferroelectric Devices* (Marcel Dekker Inc., New York 2000).
- 3 Scott J. 2000. *Ferroelectric Memories*. Berlin: Springer Verlag
- 4 S.V. Kalinin, B.J. Rodriguez, S. Jesse, E.Karapetian, E.A. Eliseev, A.N. Morozovska, *Annu. Rev. Mat. Sci.* 37: 189-238 (2007).
- 5 *Nanoscale Characterization of Ferroelectric Materials*, ed. M. Alexe and A. Gruverman (Springer-Verlag, Berlin 2004).
- 6 S. V. Kalinin, B. J. Rodriguez, S. Jesse, J. Shin, A. P. Baddorf, P. Gupta, H. Jain, D. B. Williams, and A. Gruverman, *Microscopy and Microanalysis* 12, 206-20 (2006).
- 7 Y. Cho, S. Hashimoto, N. Odagawa, K. Tanaka and Y. Hiranaga, *Nanotechnology* 17, S137 (2006)
- 8 S. V. Kalinin, D. A. Bonnell, T. Alvarez, X. Lei, Z. Hu, J. H. Ferris, *Nano Lett.* 2, 589-93 (2002).
- 9 B.J. Rodriguez, A. Gruverman, A.I. Kingon, R.J. Nemanich, and O. Ambacher, *Appl. Phys. Lett.* 80, 4166 (2002).
- 10 B. J. Rodriguez, S. Jesse, S. V. Kalinin, J. Kim, S. Ducharme, and V. Fridkin, *Appl. Phys. Lett.* 90, 122904 (2007).
- 11 S.V. Kalinin, B.J. Rodriguez, S. Jesse, T. Thundat, and A. Gruverman, *Appl. Phys. Lett.* 87, 053901 (2005).